Kikuchi Diffraction

19

CHAPTER PREVIEW

In this chapter and the following two, we will discuss two special cases of electron diffraction. In the first we find that inelastically scattered electrons give rise to arrays of lines in DPs known as Kikuchi patterns. In the second, we will form DPs with a convergent rather than a parallel beam. These two techniques have a lot in common. In the first, the electrons are initially being scattered by the atoms in the crystal so that they "lose all memory of direction." We can then think of these electrons as traveling in different "incident" directions. When the direction is appropriate, these electrons can be scattered again, this time by Bragg diffraction. In the second technique we use a convergent beam intentionally to make the electrons incident on the crystal over a range of different angles. In this case we have another advantage in that we can focus the beam on a much smaller area of the specimen than in SAD.

In this chapter we will show that these Kikuchi patterns can be used to give us accurate information on the beam direction and can give a direct link in reciprocal space to the stereographic projection. The topics we'll cover are basically experimental. The ideas developed here will carry over to the next two chapters when we discuss HOLZ lines.

D. B. Williams et al., *Transmission Electron Microscopy*

Kikuchi Diffraction

19

19.1. THE ORIGIN OF KIKUCHI LINES

The reason we form Kikuchi patterns is that, if the specimen is thick enough, we will generate a large number of scattered electrons which travel in all directions; i.e., they have been *incoherently* scattered but not necessarily *inelastically* scattered. They are sometimes referred to as diffusely scattered electrons. These electrons can then be Bragg diffracted by the planes. The rest of the story is geometry.

We'll discuss a little of the theory in Section 19.5, but for now we'll note the experimental facts.

- Since energy losses are small compared to E_0, the diffusely scattered electrons have the same λ as the incident electrons. This assumption holds as long as the specimen is not too thick.
- When first formed, most of the diffusely scattered electrons travel close to the direction of the incident beam. We learned in Chapter 3 that inelastic scattering is "peaked in the forward direction."
- The ideal specimen thickness will be such that we can see both the spot pattern and the Kikuchi lines as illustrated in Figure 19.1. This is one of the few situations when thinner is not necessarily better.
- Kikuchi (1928) described this phenomenon before the development of the TEM; it can occur in any crystalline specimen.

Diffuse scattering will again be important when we discuss image formation in Chapter 31. We can select a region of reciprocal space containing diffusely scattered electrons to form the image and these electrons can be separated from the inelastically scattered electrons with an energy filter (see Chapter 40). The specimen needs to be thick enough, but if it is too thick then there will be no lines because inelastic scattering then dominates and there is no subsequent Bragg diffraction of these electrons.

19.2. KIKUCHI LINES AND BRAGG SCATTERING

The geometry of Kikuchi patterns can be understood from Figure 19.2, which relates what happens in the specimen to what you see in the DP. We imagine (Figure 19.2A) that electrons have been generated at the point shown and scatter in all directions (but mainly forward). Some of these electrons will travel at an angle θ_B to the $hk\ell$ planes as shown in Figure 19.2B and then be Bragg diffracted by the planes. Since the scattered electrons are traveling in all directions, the diffracted beam will lie on one of two cones (Figure 19.2C). In other words, we see cones of diffracted electrons rather than well-defined beams because there is a range of incident **k**-vectors rather than a single **k**-vector. Construct the cones by considering all the vectors oriented at angle θ_B to the $hk\ell$ plane; these are called *Kossel cones*. There is a pair of Kossel cones for $\pm\mathbf{g}$, another pair for $\pm 2\mathbf{g}$, and so on.

What we see in the DP is the intersection of these two cones with the screen.

Since the screen is flat and nearly normal to the incident beam, the Kossel cones appear as parabolas. If we consider regions close to the optic axis, these parabolas look like two parallel lines: the pair of Kikuchi lines. We'll sometimes refer to this pair of lines as a Kikuchi band to include the lines and the region between them; the contrast associated with the region between the lines is actually more complex (see Section 19.6).

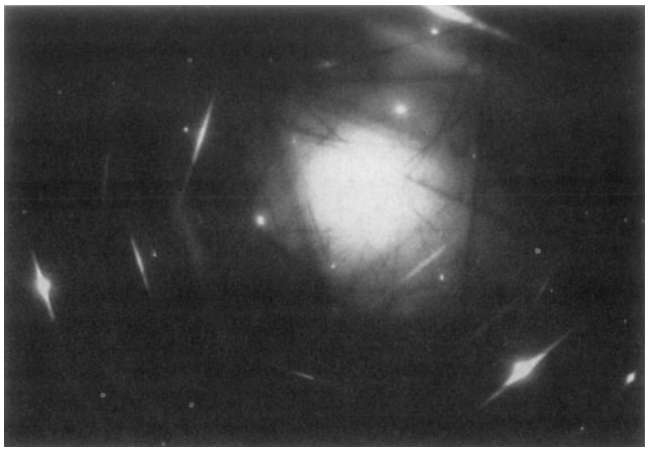

Figure 19.1. An ideal diffraction pattern containing both well-defined spots and clearly visible pairs of bright and dark Kikuchi lines.

For any pair of Kikuchi lines, one line corresponds to θ_B and the other to $-\theta_B$; one is the **g** Kikuchi line and the other the $\bar{\mathbf{g}}$ Kikuchi line. Neither of them is the **0** Kikuchi line.

We can make another important observation on the intensity of these lines by considering Figure 19.2 again. In Figure 19.2B you can see that the beam which was initially closest to the optic axis, and therefore the more intense, is further away after being scattered. This beam then gives the excess line and the other the deficient line. We can see that this simple idea really does work in Figure 19.1.

The value of this result is apparent when we want to index a pair of Kikuchi lines: if you find a bright line, its partner must not only be parallel to it but must also be closer to O, and dark.

The cones shown in Figure 19.2C act as if they are rigidly fixed to the plane $hk\ell$; they are thus fixed to the crystal. We can draw a line halfway between the two Kikuchi lines to represent the trace of the plane $(hk\ell)$. Remember our angles are all small. This simple observation explains why we have a whole chapter on Kikuchi lines. If we tilt the crystal through a very small angle, the Kikuchi lines will move but the intensities of the diffraction spots will hardly change and the *positions* of the spots will not change. The location of the Kikuchi line will also tell us whether **s** is positive or negative. We can't usually deduce that from the spot pattern.

The distance in reciprocal space between the $\bar{\mathbf{g}}$ and **g** Kikuchi lines is **g** (not 2**g**) because the angle between the two Kossel cones is $2\theta_B$.

- When the **g** Kikuchi line passes through the reflection G, $\mathbf{s}_g = 0$ (the Bragg condition is satisfied), and the $\bar{\mathbf{g}}$ Kikuchi line passes through O.

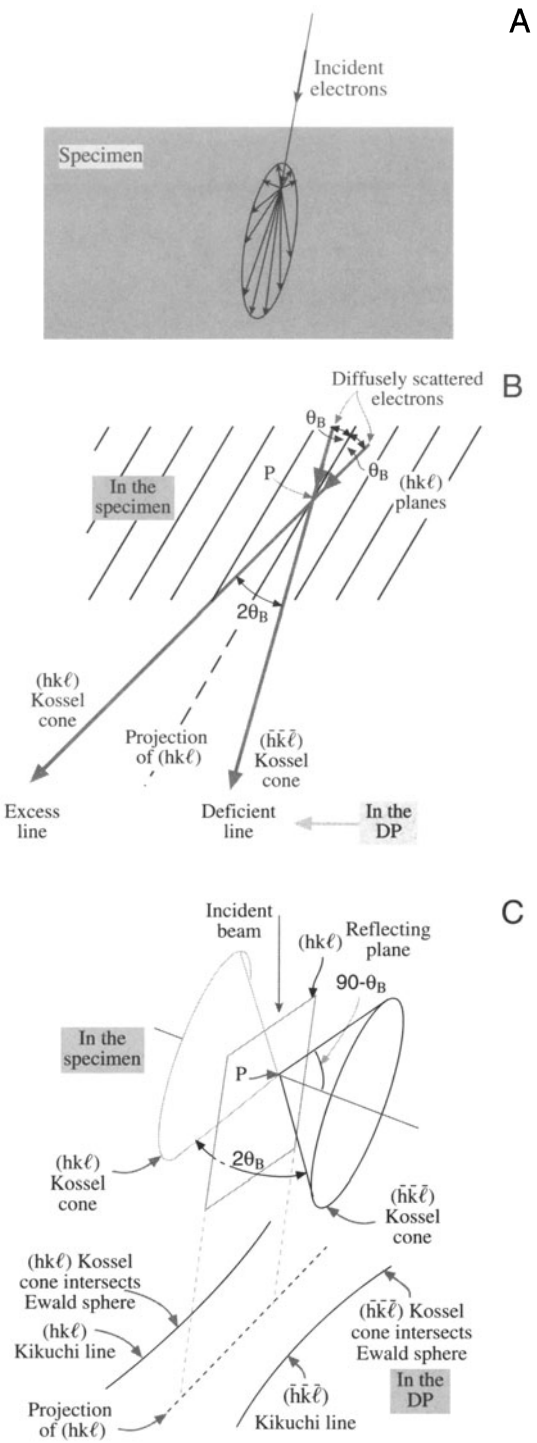

Figure 19.2. (A) Schematic representation of all electron scattering localized at a single point in the specimen. In (B) some of the scattered electrons are diffracted because they travel at the Bragg angles θ_B to certain $hk\ell$ planes. The diffracted electrons form Kossel cones centered at P on the diffracting planes. The lines closest to the incident beam direction are dark (deficient) and the lines furthest away from the beam are bright (excess). In (C) the cones intercept the Ewald sphere, creating parabolas which approximate to straight Kikuchi lines in the diffraction patterns because θ_B is small.

- A corollary: if the direct beam is exactly parallel to the plane $hk\ell$, the **g** and $\bar{\mathbf{g}}$ Kikuchi lines are symmetrically displaced about O with **g** "passing through" **g**/2 and $\bar{\mathbf{g}}$ "passing through" $\bar{\mathbf{g}}$/2.

In this latter case, our simple explanation breaks down because it would predict equal intensity in both excess and deficient Kikuchi lines, and thus they would both be indistinguishable from the diffuse-scattered background. Therefore, no Kikuchi lines should be visible if the beam is exactly down a zone axis, and this is not true. So the full Kikuchi line explanation is more complex and requires Bloch-wave theory.

19.3. CONSTRUCTING KIKUCHI MAPS

The method for constructing Kikuchi maps is illustrated in Figure 19.3. We draw the lines for the case where the [001] pole is exactly on the optic axis. The lines are then the perpendicular bisectors of every **g**-vector you can find in the ZOLZ. The distance between each pair of lines is then automatically |**g**|. We can then give each line a unique label **g**.

Next, we can construct the map for the [101] pole. We start as shown in Figure 19.4, keeping the common 020 **g**-vector pointing in the same direction. So, the 020 and 0$\bar{2}$0 Kikuchi lines are common to the two patterns. Although the angle between the [001] and [101] poles is 45°, we draw the 020 lines as parallel and straight because we are always looking at a small segment of the Kikuchi pattern. Notice that we can define all the distances in terms of their equivalent angles, as in any DP.

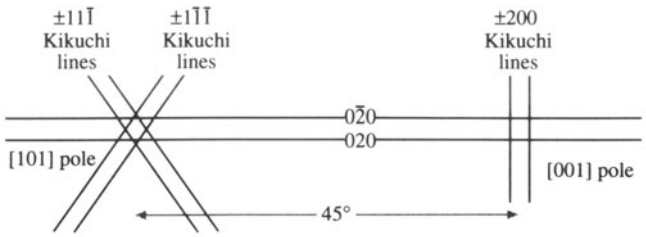

Figure 19.4. From one Kikuchi pattern we can extend the lines to create a second pattern. For example, knowing the [001] pattern we can construct the [101] pattern since a pair of lines is common to both. So we draw the 0$\bar{2}$0 and 020 lines from the [001] pole 45° to the [101] pole.

Now we add the [112] pattern. This pattern shares the 2$\bar{2}$0 and $\bar{2}$20 reflections with the [001] pole and shares the $\bar{1}\bar{1}$1 and 11$\bar{1}$ reflections with the [101] pole. The corresponding pairs of Kikuchi lines will then also be common, so we produce the triangle shown in Figure 19.5A. We can add other poles and pairs of Kikuchi lines as shown in Figure 19.5B.

It's a good exercise to construct a Kikuchi map for your material as illustrated for the fcc case in Figure 19.6. The maps are available in the literature for fcc, bcc, diamond-cubic, and some hcp materials. Such maps are mainly from Thomas and co-workers (Levine *et al.* 1966, Okamoto *et al.* 1967, Johari and Thomas 1969), who developed the technique. Maps can also be downloaded from the WWW using EMS.

You can appreciate the value of Kikuchi maps in noncubic materials from the map shown in Figure 19.7. The map has been drawn for Ag_2Al, which has the same *c/a* ratio as Ti. The Kikuchi bands are labeled: they correspond to planes. The zone axes are also labeled: they correspond to directions. Thinking back to our brief discussion of Frank's paper on four-index notation in Chapter 16, you can see an obvious application here.

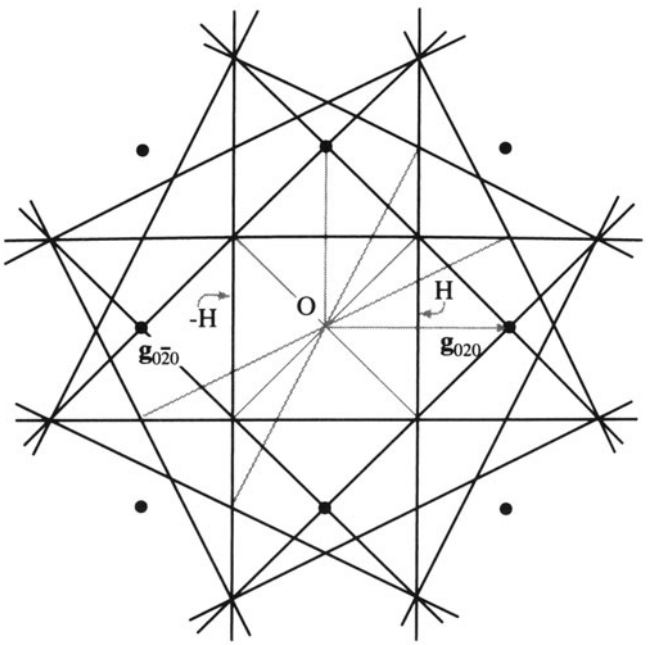

Figure 19.3. To construct a Kikuchi pattern, draw pairs of lines each bisecting the ±**g** vectors. For example, when the [001] fcc pole is on axis, the vector $\mathbf{g}_{020}$ is bisected by the vertical line at H and the companion Kikuchi line is at -H (0$\bar{2}$0). All other Kikuchi line pairs can be constructed for any **g**-vector.

- For cubic materials you need only the [001], [101], [111] triangle shown in Figure 19.5B.
- For hcp materials, the angles will generally depend on the *c/a* ratio of your material and you'll need a larger area of the map.
- For most noncubic materials and particularly if you are working with monoclinic or triclinic crystals, it's not practical to construct the com-

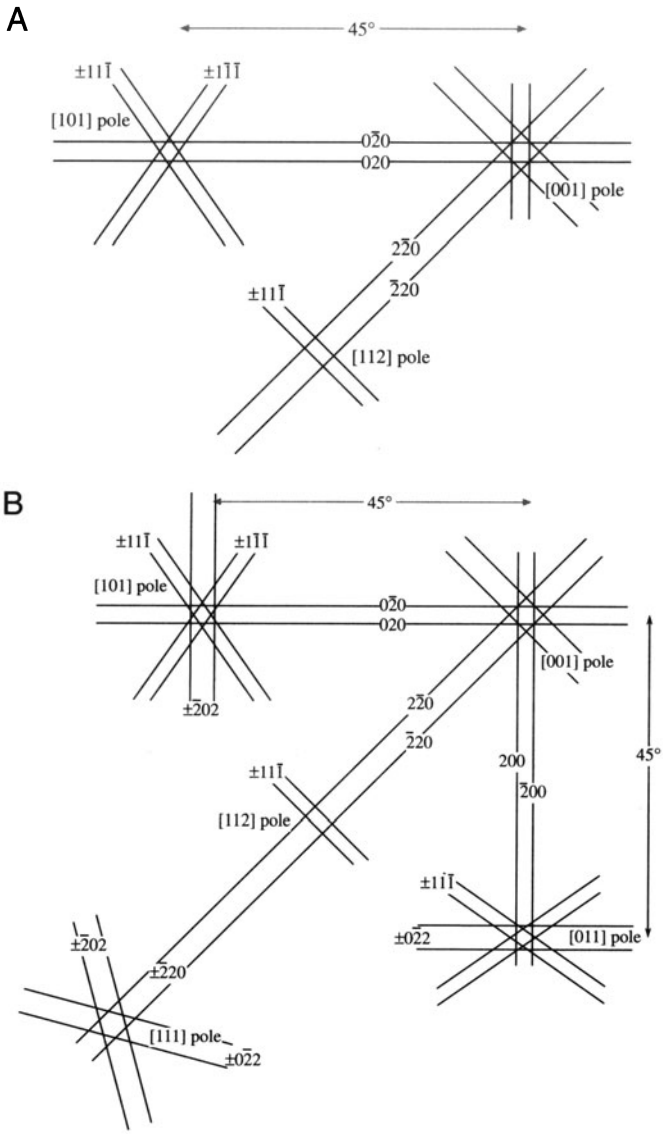

Figure 19.5. (A) Construction of the [112] pattern from the [001] and [101] patterns by extending the Kikuchi lines common to each pair of patterns. The [11$\bar{1}$] pair is common to the [101] and [112] patterns and the $\bar{2}$20 pair is common to [001] and [112] patterns. (B) Other poles can be added such as [011] and [111]. Note that the Kikuchi line pairs are not straight lines connecting poles. They are curved because over large angles their parabolic shape is evident. Nevertheless we draw them as straight lines where possible.

plete map experimentally. It's probably easier to become a metallurgist!

We can use the following procedure to generate a valuable experimental aid for any material:

- Construct segments of the map to scale as we've illustrated in Figure 19.5B. You can use one of the software packages to help you in this task. Make two copies of each map.

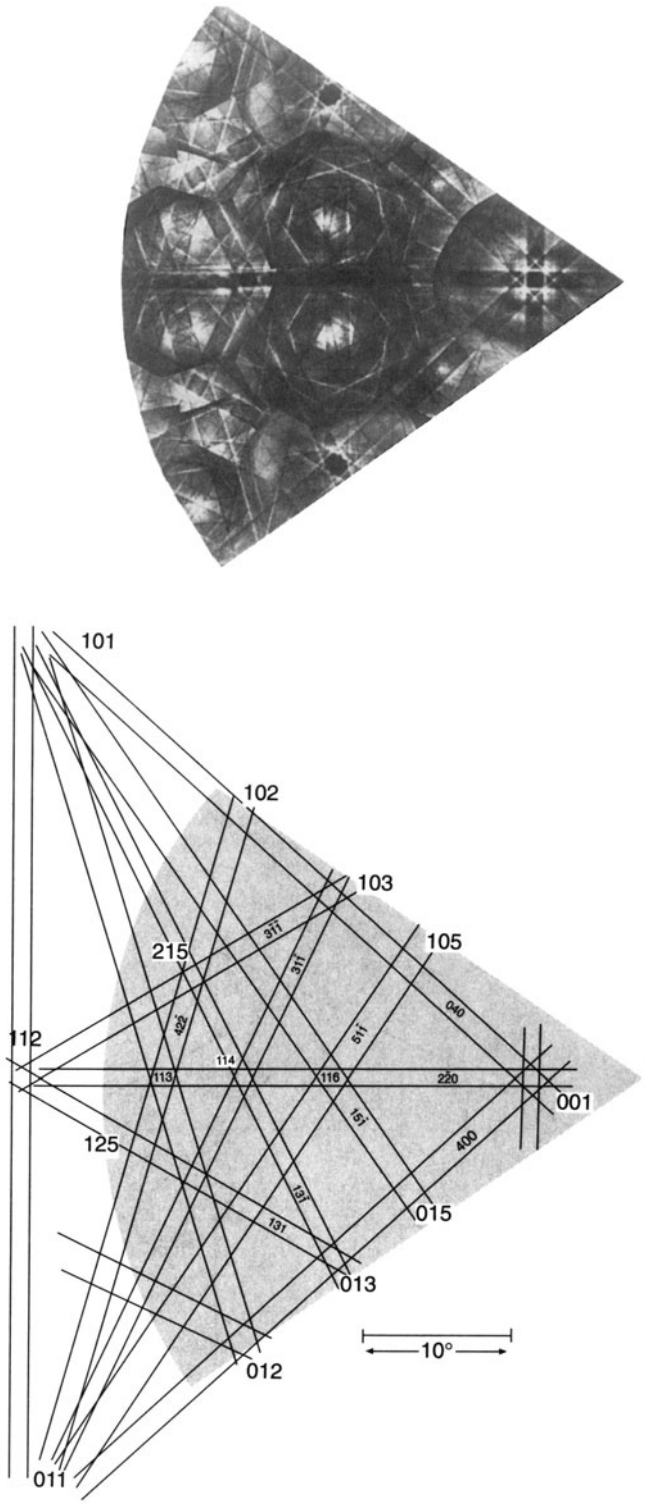

Figure 19.6. (A) Experimental Kikuchi map for fcc crystals and (B) indexed Kikuchi lines in the schematic map.

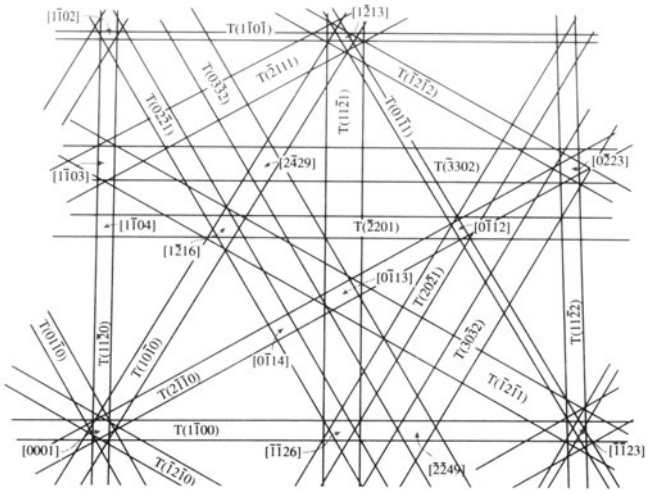

Figure 19.7. Part of the schematic Kikuchi map for hexagonal Ag_2Al with the principal poles and pairs of lines indexed.

- At the TEM, record the Kikuchi pattern for several special low-index poles along with the spot pattern.
- Index the DPs consistently.
- Print DPs for each pole at the scale you used in your line drawing of the Kikuchi map.
- Now add the experimental patterns to the line diagrams and you have two very useful experimental aids. An illustration is given in Figure 19.8.

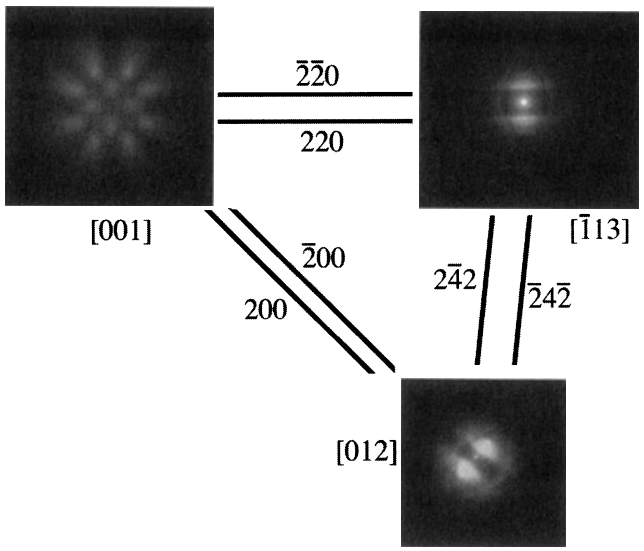

Figure 19.8. Experimental Kikuchi patterns around three principal poles in MgO with the common Kikuchi lines between each pole drawn in. You should compare this figure with the diffraction patterns in Figure 18.7.

When discussing Kikuchi maps, we like to use the road-map analogy. (Repeatedly!) What we just recommended is that you record the maps of the towns with pictures so that you'll recognize them. When you're on the highway traveling from town to town, you don't much care what the road looks like although you do want to know how far you've traveled and how much further you have to go.

By now you will appreciate even more the value of the stereographic projection we introduced in Chapter 18. Use the stereographic projection and the Kikuchi map together. The stereographic projection concisely summarizes all the relative locations of all the plane normals and the zone axes. Use the stereographic projection to relate Minneapolis and London, but use the Kikuchi map to locate the Guthrie Theater and Buckingham Palace.

19.4. CRYSTAL ORIENTATION AND KIKUCHI MAPS

In Chapter 18 we showed how you could estimate the orientation of the beam relative to the crystal with an accuracy of ~3°. Using Kikuchi patterns we can increase this accuracy to ~0.1°.

A routine method for this determination has again been developed by Thomas and co-workers (e.g., Okamoto *et al.* 1967), who pioneered this use of Kikuchi maps. The beam direction, $[UVW]$, lies along the optic axis O in Figure 19.9. A, B, and C are major poles (i.e., zone axes), which we can determine by observation and measurement. Let the indices of A = $[p_1\ q_1\ r_1]$, B = $[p_2\ q_2\ r_2]$, and C = $[p_3\ q_3\ r_3]$. Having indexed these poles you can check your result by measuring the angles α, β, and γ between the traces of the planes in Figure 19.9A (which equals the angle, ϕ, between the plane normals in all systems); calculate each angle using equation 18.3 if your material is cubic.

Measure the distances OA, OB, and OC in Figure 19.8 and, using the calibrated camera length, convert these distances into angles, ρ_1, ρ_2, and ρ_3 (which are defined in Figure 19.9B). If $[UVW]$ is the direction of the beam, then we can use the same vector dot product approach (equation 18.4 for the cubic case) to give equations for ρ_1, ρ_2, and ρ_3. Notice we are distinguishing between ρ and ϕ (see Section 18.4). The angles α, β, and γ in Figure 19.9A are slightly distorted values of $(90 - \phi)$.

You can solve these three equations for the three unknowns U, V, and W and hence we have **B**. Finally, always check the sign of **B**, as we described in Section 18.8.

It is possible that the DP you have to work with is not obviously near a zone axis. Normally, while you are at

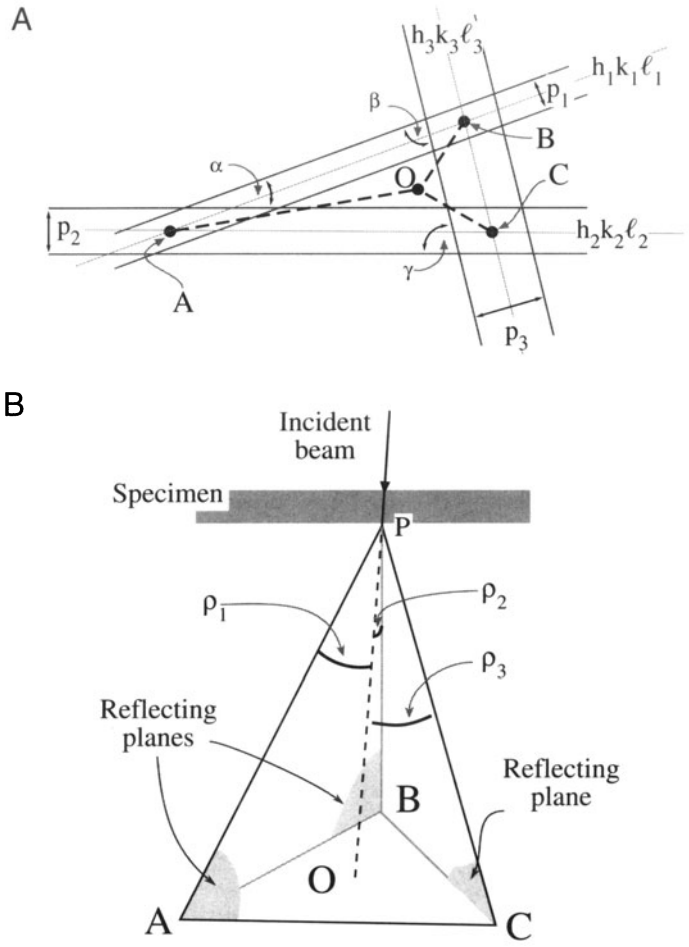

Figure 19.9. In (A) pairs of Kikuchi lines from the reflecting planes also intercept at points A, B, C. The distances from O to the points A, B, C correspond to the angles between the beam direction and the three zone axes while the angles α, β, γ correspond to the angles between pairs of plane normals. The angle α is between the $(h_1k_1\ell_1)$ and $(h_2k_2\ell_2)$ plane normals, etc. (B) Three reflecting planes in the specimen with traces AB $(h_1k_1\ell_1)$, AC $(h_2k_2\ell_2)$, and BC $(h_3k_3\ell_3)$ around the direct beam, O. The traces of pairs of planes intercept at A (AB, AC), B (AB, BC), and C (AC, BC).

the microscope, you will tilt along the different Kikuchi bands until you find the appropriate poles to ease your task later. All is not lost if you can just find pairs of Kikuchi lines as shown in Figure 19.10. If you see an excess line you will find the deficient line quite easily. Now trace these lines in both directions and you will find the poles. Use your knowledge of the *d*-spacings to index the pairs of Kikuchi lines. Remember that the zone axis lies parallel to each plane so it's defined by where the two plane traces meet. Now if you can index three poles, you can obtain **B**, as in Figure 19.9.

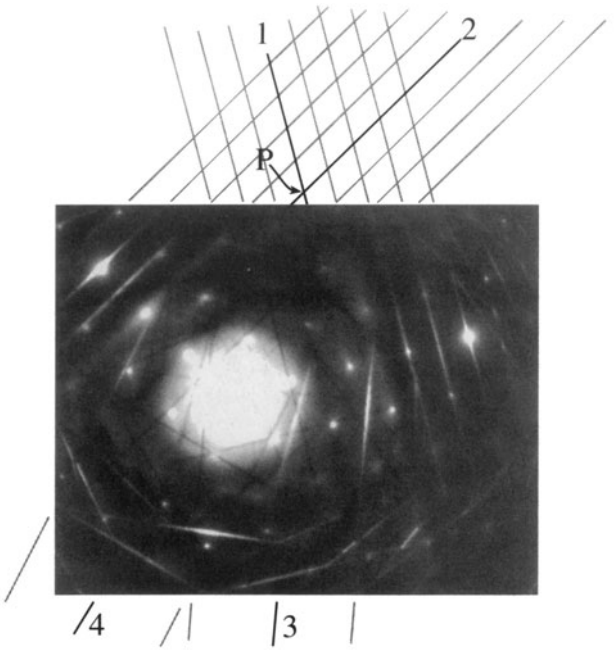

Figure 19.10. To index a diffraction pattern well away from a low-index zone axis, extend the Kikuchi lines. The dark lines 1–4 represent the traces of the diffracting planes which intercept at a pole (P). For Kikuchi lines 1 and 2 the higher-order extensions are also drawn. From the *d*-spacings, index the Kikuchi line pairs. The angles between the beam direction and the poles, P, can then be measured directly.

19.5. SETTING THE VALUE OF s_g

Since the Kikuchi lines are "rigidly attached" to the crystal, they give us a very accurate measure of the excitation error $\mathbf{s}_g$. The diffraction geometry is shown in Figure 19.11 following Okamoto *et al.* (1967). When $\mathbf{s}_g$ is negative, the **g** Kikuchi line is on the same side of **g** as O; when $\mathbf{s}_g$ is positive, the line lies on the opposite side of **g**. For high-energy electrons, and knowing the camera length *L*, we can write an expression for the angle η

$$\eta = \frac{x}{L} = \frac{x\lambda}{Rd} \qquad [19.1]$$

where *d* is $|\mathbf{g}|^{-1}$. The distances *x* and *R* are measured on the photographic negative.

The angle ε is given by

$$\varepsilon = \frac{s}{g} \qquad [19.2]$$

Now we can set $\varepsilon = \eta$, to give

$$s = \varepsilon g = \frac{x}{L}g = \frac{x}{Ld} \qquad [19.3]$$

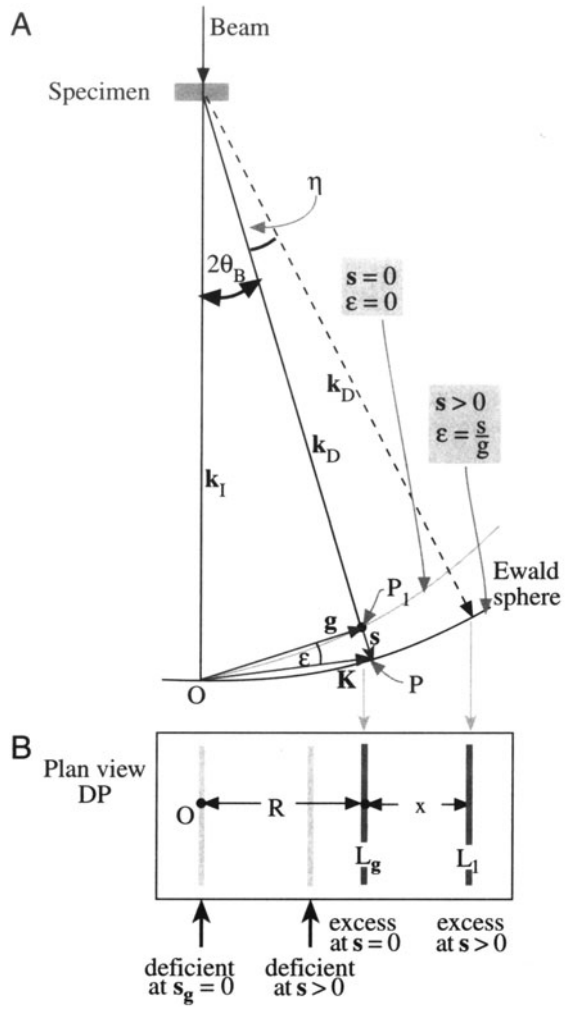

Figure 19.11. (A) The distance between the diffraction spot and its Kikuchi line gives a direct measure of **s**. The angle ε is *s*/*g* and is zero at the exact Bragg condition. (B) Measure x, the spacing between O and the deficient line (or G and the excess line), to determine **s**.

Again, with our small-angle approximation, the distance between the excess and deficient Kikuchi lines, R, (the distance g measured on the DP) is equivalent to $2\theta_B L$. So using Bragg's Law, we have

$$\frac{R}{L} = 2\theta_B = \frac{\lambda}{d} \qquad [19.4]$$

Hence the expression for s is

$$s = \frac{x}{Ld} = \frac{x}{d} \cdot \frac{\lambda}{Rd} \qquad [19.5]$$

$$s = \frac{x}{R}\frac{\lambda}{d^2} = \frac{x}{R}\lambda g^2 \qquad [19.6]$$

We'll reconsider this equation when we discuss weak-beam microscopy in Chapter 26.

Ryder and Pitsch (1968) have given a method for determining **B** using the approach we described in Section 19.4 with the accuracy given by equation 19.6. Their expression for **B** is

$$\mathbf{B} = \alpha_1 |\mathbf{g}_1|^2 (\mathbf{g}_2 \times \mathbf{g}_3) + \alpha_2 |\mathbf{g}_2|^2 (\mathbf{g}_3 \times \mathbf{g}_1) + \alpha_3 |\mathbf{g}_3|^2 (\mathbf{g}_1 \times \mathbf{g}_2) \qquad [19.7]$$

where α_i is given by

$$\alpha_i = \frac{R_i + 2x_i}{R_i} \qquad [19.8]$$

where R and x are defined in Figure 19.11.

19.6. INTENSITIES

We'll conclude with a few remarks for further thought:

- Tan *et al.* (1971) have shown experimentally that the distance between a pair of Kikuchi lines may change at larger specimen thicknesses due to dynamical scattering.
- Kikuchi lines can also be produced by the backscattered electrons. In the SEM these patterns are simply known as electron-backscatter patterns or EBSPs. They were regarded as a curiosity until it was shown (Dingley *et al.* 1992, Randle 1993) that you can rapidly map out the texture of polycrystalline materials using these patterns, without thinning the sample. New detection systems, similar to the YAG- or CCD-based cameras, and some fast computer algorithms have led to the development of "orientation imaging" in the SEM. Similar techniques should be available for TEM Kikuchi maps. They won't be as automated, but TEM can give the interface plane much more accurately so the two techniques will be complementary.
- In the next chapter we'll discuss HOLZ lines; HOLZ lines are very closely related to Kikuchi lines but are a little more complicated, since the Bragg planes are always inclined to the direct beam.
- In Chapter 23 we'll discuss ZAPs, or zone-axis patterns, in images; these ZAPs are, in many respects, the real-space version of Kikuchi lines. However, you should remember that their physical origin is *completely different*; the most im-

portant features of ZAPs are *not* associated with incoherent, inelastic, or diffuse scattering.

- Bloch waves with vector $\mathbf{k}^1$, for example, are more strongly scattered than those corresponding to branch 2 of the dispersion surface. Therefore, we can expect anomalous absorption (see Chapter 23) to influence the intensity of Kikuchi patterns. Such effects do in fact lead to excess and deficient Kikuchi bands. Since we haven't yet found any use for the information in these bands we'll refer you to Reimer (1993) for further reading.
- We mentioned earlier that the contrast between the lines, i.e., the band, is complex. The contrast is actually strongly influenced by anomalous absorption of the Bloch waves which are formed by coherent scattering of the incoherently scattered electrons; so all is clear.
- There are strong similarities between the Kikuchi process and the operation of a monochromator in optics: both select and diffract a particular wavelength or frequency.
- You can appreciate that the scattering is quite complex by considering what happens when the diffracting plane is exactly parallel to the incident beam: the two Kikuchi lines will both be visible although you might have guessed otherwise.

Back in Chapter 6 we noted that electron ray paths rotate through the objective lens field, but in all our discussion of diffraction (including Kikuchi lines and the following CBED patterns) we draw all the electron paths as straight lines, ignoring any rotation. However, particularly in a modern condenser-objective lens TEM, the lens field is relatively strong and can introduce a significant rotation into the off-axis incident and diffracted electrons. An interesting consequence of this effect is that Kikuchi lines in modern TEMs may be less sharp than in older TEMs, unless you illuminate only a very small area of the specimen. If you're intrigued by this then you must read "Skew thoughts on parallelism" by Christenson and Eades (1988).

CHAPTER SUMMARY

- The Kikuchi lines consist of an excess line and a deficient line. In the DP, the excess line is further from the direct beam than the deficient line.
- The Kikuchi lines are fixed *to the crystal* so we can use them to determine orientations accurately.
- The trace of the diffracting planes is midway between the excess and deficient lines.
- We can determine the value of $\mathbf{s}_g$ by measuring the separation between the **g** Kikuchi line and the G reflection (the separation is 0 when $\mathbf{s}_g = 0$).

Pairs of Kikuchi lines define the road. Taken together, the roads make up a map. The rule is different than road maps: in our maps, narrow roads are the most important! What is the relevance of the roadside curbs? They define the roads and tell us when we are standing on them, but we are not too interested in their detailed appearance. We view Kikuchi maps as an invaluable tool for the microscopist.

Kikuchi lines and Kikuchi maps are one of the most important aids we have when orienting, or determining the orientation of, crystalline materials. Knowing the orientation of your specimen is essential for any form of quantitative microscopy, whether you're analyzing dislocation Burgers vectors by diffraction contrast, imaging grain boundaries with lattice resolution, or measuring chemistry variations by EELS or XEDS. They are especially useful when combined with the map of zones and poles (directions and plane normals) on the stereographic projection. Use the computer to check or to assist you in constructing a map for your material.

REFERENCES

General References

Thomas, G. (1978) in *Modern Diffraction and Imaging Techniques in Material Science* (Eds. S. Amelinckx, R. Gevers, and J. Van Landuyt), p. 399, North-Holland, Amsterdam.

Specific References

Christenson, K.K. and Eades, J.A. (1988) *Ultramicroscopy* **26**, 113.

Dingley, D.J., Baba-Kishi, K., and Randle, V. (1992) *An Atlas of Electron Back-Scatter Diffraction Patterns,* Institute of Physics, Bristol, United Kingdom.

Johari, O. and Thomas, G. (1969) *The Stereographic Projection and Its Applications in Techniques of Metals Research* (Ed. R.F. Bunshah), Interscience, New York.

Kikuchi, S. (1928), *Jap. J. Phys.* **5**, 23.

Levine, E., Bell, W.L., and Thomas, G. (1966) *J. Appl. Phys.* **37**, 2141.

Okamoto, P.R., Levine, E., and Thomas, G. (1967) *J. Appl. Phys.* **38**, 289.

Randle, V. (1993) *The Measurement of Grain Boundary Geometry,* Institute of Physics, Bristol, United Kingdom.

Reimer, L. (1993) *Transmission Electron Microscopy; Physics of Image Formation and Microanalysis,* 3rd edition, Springer-Verlag, New York.

Ryder, P.L. and Pitsch, W. (1968) *Phil. Mag.* **18**, 807.

Tan, T.Y., Bell, W.L., and Thomas, G. (1971) *Phil Mag.* **24**, 417.